Ion cyclotron harmonics in the Saturn downward current auroral region

J. D. Menietti,[1] P. Schippers,[1] O. Santolík,[2,3] D. A. Gurnett,[1] F. Crary,[4] and A. J. Coates[5]

Received 23 August 2011; revised 22 November 2011; accepted 29 November 2011; published 30 December 2011.

[1] Observations of intense upgoing electron beams and diffuse ion beams have been reported during a pass by Cassini in a downward current auroral region, nearby a source region of Saturn kilometric radiation. Using the Cassini Radio and Plasma Wave Science (RPWS) instrument low frequency waveform receiver and the Cassini Plasma Spectrometer Investigation (CAPS) instrument we have been able to identify ion cyclotron harmonic waves associated with the particle beams. These observations indicate similarities with terrestrial auroral emissions, and may be a source of wave-particle interactions. We fit the observed plasma electron distribution with drifting Maxwellians and perform a linear numerical analysis of plasma wave growth. The results are relevant to ion heating and possibly to electron acceleration.

Citation: Menietti, J. D., P. Schippers, O. Santolík, D. A. Gurnett, F. Crary, and A. J. Coates (2011), Ion cyclotron harmonics in the Saturn downward current auroral region, *J. Geophys. Res.*, *116*, A12234, doi:10.1029/2011JA017102.

1. Introduction

[2] Electrostatic and electromagnetic ion cyclotron waves have been observed in the terrestrial auroral zones for many decades, [cf. *Gurnett and Frank*, 1972; *Kintner et al.*, 1978]. These waves are known to be sources of parallel electron acceleration and ion heating (conics) in the auroral zone as evidenced from more recent FAST data [cf. *McFadden et al.*, 1998; *Carlson et al.*, 1998; *Lund et al.*, 1998; *Cattell et al.*, 1998; *Chaston et al.*, 1998]. *Carlson et al.* [1998] have further reported FAST observations in the terrestrial auroral region showing a correspondence between upward electron beams, upward ion conical distributions, and enhanced electromagnetic noise. The growth of ion cyclotron waves (ICWs) has been investigated by many authors in the past. Free energy sources include electron currents [*Rosenbluth*, 1965; *Kindel and Kennel*, 1971], ion beams [*Weibel*, 1970], and loss cone distributions of energetic ions [*Ashour-Abdalla and Thorne*, 1978]. *Singh et al.* [1985] have investigated the growth of ICWs generated by electron beams. *Temerin and Lysak* [1984], *Lin et al.* [1989], and, more recently, *Chaston et al.* [2002] have all investigated the effectiveness of electron beams as a free energy source for the growth of electromagnetic ion cyclotron (EMIC) waves in the terrestrial magnetosphere. In addition, *Temerin et al.* [1986] have investigated the role of EMIC waves in modulating the flux of electrons.

[3] *Mitchell et al.* [2009] reported ion conics associated with electron beams at high latitude auroral passes of the Saturn magnetosphere. The ion conics have energies in the range from 30 keV to 200 keV, while the electron energies extend from about 20 keV to almost 1 MeV. *Mitchell et al.* [2009] have suggested these large energies may result from the much larger scale of the Saturn magnetosphere compared to Earth where electron and ion beams have peak energies <5 keV typically. On 17 October, 2008 (day 291) the Cassini spacecraft made a high latitude polar pass through the Saturn southern auroral region. *Bunce et al.* [2010] report that this pass includes both downward and upward current regions in what appears to be a period of solar wind compression. *Schippers et al.* [2011] have recently presented a detailed description of plasma observations for this same pass near a source of Saturn Kilometric Radiation (SKR) [cf. *Lamy et al.*, 2010; *Kurth et al.*, 2011]. The authors report intercepting adjacent regions of upward and downward current regions which include field-aligned electron and ion beams.

[4] *Lysak et al.* [1980] have investigated ion heating in the terrestrial auroral region due to electrostatic ion cyclotron waves. The source of the heating is both linear and nonlinear wave dispersion. At Saturn, the high energies may be a result of heating over large distances along the magnetospheric field lines as suggested by *Mitchell et al.* [2009]. It is also conceivable that a field-aligned static electric field could trap the upward ions ("pressure cooker") to increase the heating rate [cf. *Gorney et al.*, 1985], contributing to significantly more ion heating in downward current regions. In this paper we discuss observations of intense hydrogen cyclotron waves associated with upward electron beams in a downward current region on day 291 of 2008. We show that these

[1]Department of Physics and Astronomy, University of Iowa, Iowa City, Iowa, USA.
[2]Institute of Atmospheric Physics, Academy of Sciences of the Czech Republic, Prague, Czech Republic.
[3]Faculty of Mathematics and Physics, Charles University, Prague, Czech Republic.
[4]Southwest Research Institute, San Antonio, Texas, USA.
[5]Mullard Space Science Laboratory, University College London, London, UK.

0148-0227/11/2011JA017102

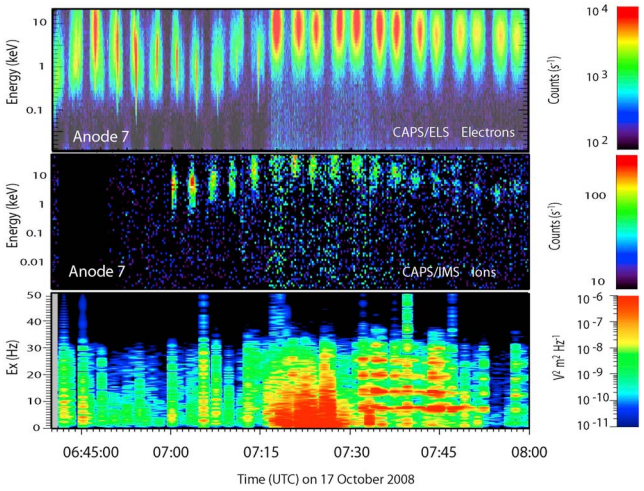

Figure 1. Spectrograms of the downward current region observed from about 06:40 to 08:00 UT on day 291 of 2008. (top) The electron and (middle) ion data (CAPS) and (bottom) the wave electric field observations (0–25 Hz) from the low frequency Waveform Receiver. Upward electron beams and weaker ion beams are observed for t < 07:15, but in the interval 07:15 < t $\lesssim$ 07:45 the electron beams intensify by about an order of magnitude while the ion beams first increase in energy but then become weak and diffuse. Hydrogen cyclotron harmonics are observed by the WFR as seen in the bottom illustration.

waves can be generated by the electron beams, and may be responsible for at least some of the ion heating.

2. Observations

[5] In Figure 1 we present a spectrogram of the downward current region observed from about 06:40 to 08:00 UTC on day 291 of 2008. During this pass, intense upward electron and ion beams were observed (due to operational limitations, particle pitch angles, $\alpha \lesssim 20°$, were not sampled by the Cassini Plasma Spectrometer Investigation (CAPS)). Details of the Cassini CAPS, which includes the Electron Spectrometer (ELS), the Ion Beam Spectrometer (IBS), and the Ion Mass Spectrometer (IMS) are reported by *Young et al.*, 2004. The top two panels display the electron and ion data (CAPS) and the lower panel shows the wave electric field from the low-frequency (0–25 Hz) Waveform Receiver (WFR) on board Cassini. The WFR is one of five receiver systems on the Radio and Plasma Wave Investigation (RPWS). It is a five channel receiver that covers the frequency range from 1 Hz to 2.5 kHz in two bands, 1 Hz to 25 Hz and 3 Hz to 2.5 kHz. For this study only the lower band is presented. Upward electron beams and weaker ion beams are observed for t < 07:15, but in the interval 07:15 < t $\lesssim$ 07:45 the electron beams intensify by about an order of magnitude and extend above the maximum energy of the ELS, while the ion beams first increase in energy but then become weak and diffuse and extend to energies of ~10 keV [cf. *Schippers et al.*, 2011]. At the same time the wave electric fields indicate ion cyclotron harmonics. These waves appear as constant-frequency bands of emission with lowest frequency near the local hydrogen cyclotron frequency (~6 Hz) and at least 3 harmonics in the approximate time range 07:31 < t < 07:52. After this time the ion cyclotron waves (ICWs) become weak. There is a gap in the spectra from approximately 07:53 to 07:57 which may be due to the orientation of the Ex antenna.

[6] In Figure 2 we re-plot the WFR data for the time interval 07:15 to 08:00 displaying the data for each receiver. The top two panels show the electric field intensity and the bottom three panels show the magnetic field intensity. The fundamental and up to three harmonics are observed in the E-field data. Unfortunately the B-field data is much noisier and possible signatures near the frequencies of the electric field harmonics are also near interference resonance frequencies of the B-field receiver. In Figure 3 we display a snapshot of the electric field waveform for a 5 s period starting at 07:37:22. It is clear that large amplitude signatures are seen during the entire period. The frequency of these waves is about 6 Hz, near the total hydrogen cyclotron frequency, and the intensity levels sometimes reach over 5 mV/m. Contours of the electron phase space distribution function are displayed in $v_{\parallel}$ and $v_{\perp}$, in Figure 4 (middle) for the time period 07:37:36 during the time of the observation of the ICWs. The gaps in the plot indicate no data is available. Note there is no coverage for the downgoing electrons. The upper panel shows line plots of the electron distribution

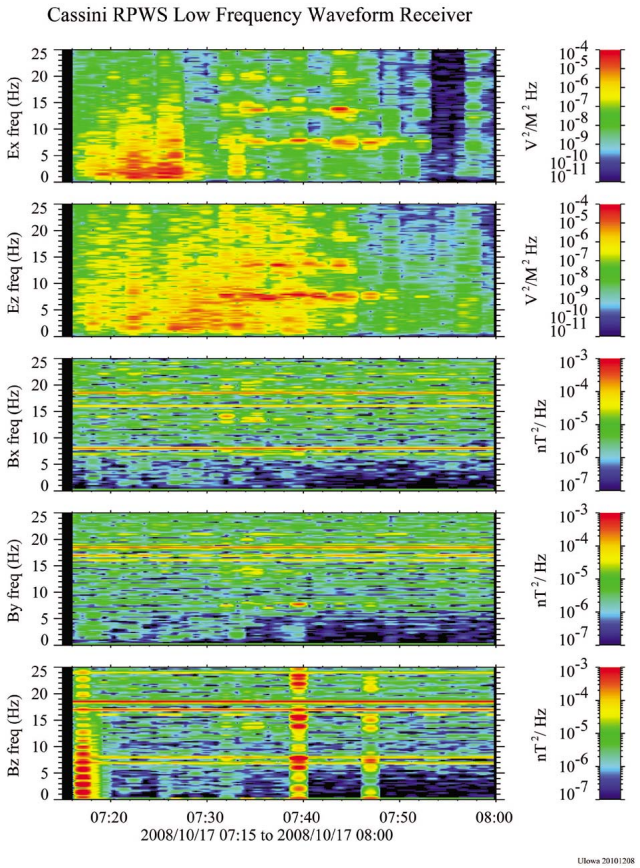

Figure 2. The WFR data is re-plotted for the time interval 07:15 to 08:00 displaying the data for each receiver. The first two panels show the electric field intensity and the last three panels show the magnetic field intensity. The fundamental and up to three harmonics are observed in the E-field data.

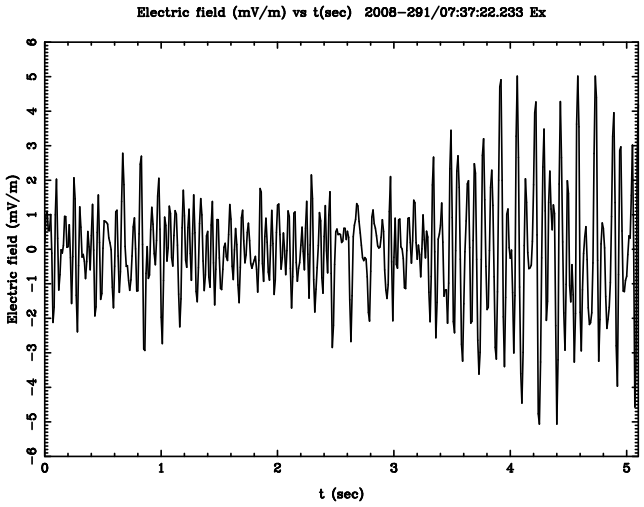

Figure 3. A snapshot of the electric field waveform for a 5 s period starting at 07:37:22. It is clear that large amplitude signatures are seen during the entire period, especially between seconds 3 to 5.

function and indicates significant upward beams near 100 eV for the anode intercepting the parallel energy axis. In Figure 4 (bottom) we plot a two-dimensional smoothed version of the observed distribution showing the extent of the suprathermal tail of the ion beam. The distribution at pitch angles where we have no data (lowest pitch angles) is obtained by extrapolation of the observed distribution.

[7] We have estimated the growth of the observed ICWs using a dispersion solver, WHAMP, waves in homogeneous, anisotropic multicomponent plasmas [*Ronnmark*, 1982, 1983]. We model the electron phase space distribution (PSD) using a sum of drifting Maxwellians for each of six plasma components. These components include a core electron distribution, beam electron component, and extended tail beam electron component. There is also a cold, core Maxwellian ion plasma distribution for charge neutrality. The electron cyclotron frequency is f_c = 10.6 kHz, the plasma frequency, f_p = 1.3 kHz, consistent with plasma moment calculations reported by *Schippers et al.* [2011]. Table 1 lists the parameters used in the calculations, where $w_{\|}$ is the parallel (to magnetic field) thermal energy and v_d is the parallel drift velocity. The free energy source for the ICWs is the electron beam with $V_d = 6.15 \times 10^6$ m/s. In Figure 5 (top) we show a plot of the observed (dashed) and model (dot-dash) distribution for a pitch angle of 180° (beam direction). Note that spacecraft charging effects are present in the observed distribution for $v_{tot} \lesssim 3 \times 10^6$ m/s, so the ramped distribution observed for the lowest energies is not the actual. Figure 5 (bottom) shows a blow-up of Figure 5 (top) near the region of the beam responsible for the growth of the ICWs near 6.1×10^6 m/s. The results of the wave growth analysis are plotted in Figure 6 for the fundamental and 3 harmonic frequencies. The growth rates are relative to the fundamental hydrogen cyclotron frequency (f_H = 5.77 Hz). The fundamental waves at $f \sim f_{ci}$ have a weak magnetic component, with $cB/E \sim 1.43$, and $k_{\perp}/k_{\|} \sim 1.71$. The harmonic waves are much more electrostatic, with oscillating $B \sim 0$. We can estimate the relative gain of the emission. From Figure 2 we see that

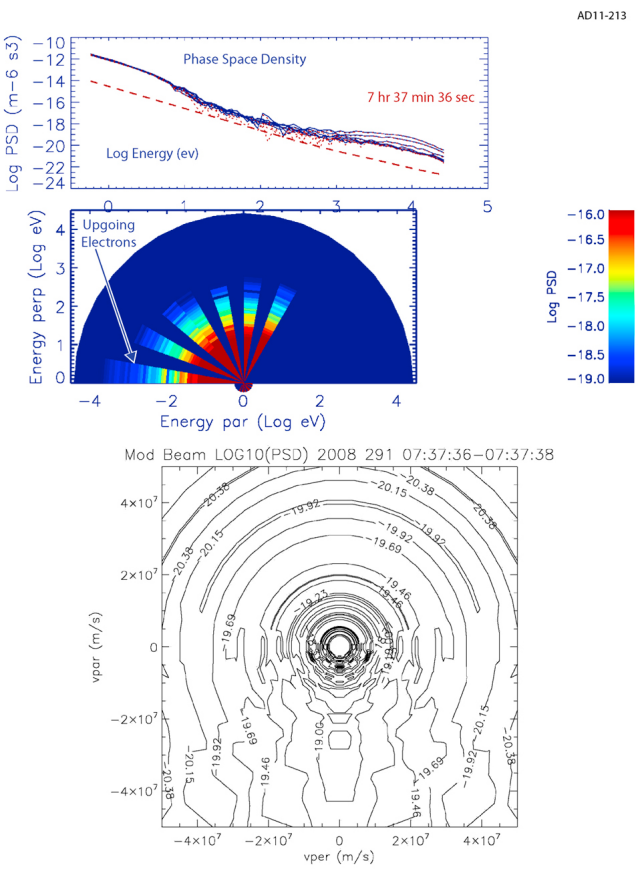

Figure 4. (top) Line plots of the electron distribution function for each anode, indicating significant upward beams near 100 eV. (middle) Contours of the electron phase space distribution function in $v_{\|}$ and $v_{\perp}$, for the time period 07:37:36 during the time of the observation of the ICWs. The gaps in the plot indicate no data is available. Note there is no coverage for the downgoing electrons. (bottom) We plot a two-dimensional contour of the observed distribution. The distribution at pitch angles where we have no data ($v_{\|} > 0$) is obtained by extrapolation of the observed distribution for a pitch angle of 75°.

the ICWs grow by 5 to 6 orders of magnitude in intensity. We write the power gain as $P/P_o = e^{2g}$, where $g = \omega_i\, dt = \omega_i\, (l/v_g)$, where ω_i is the wave growth rate and v_g is the wave group velocity. From the wave linear dispersion analysis (cf. Figure 6) the maximum growth rate for fundamental emission $\omega_i = 1.23\ s^{-1}$, v_g = 7.56 km/s (perpendicular to B), so we find $g = 1.63 \times 10^{-4}\ l$. For the case of 6 orders of

Table 1. Plasma Parameters for Growth Rate Calculations of ICWs

Component	Density (m^{-3})	$w_{\|}$(eV)	$T_{\perp}/T_{\|}$	$v_d(10^7$ m/s)
Cold electron (core)	5.29×10^3	0.2	1.0	0.0
Warm electron	1.3×10^1	1.15	3.0	0.45
Warm electron (beam)	1.2×10^1	0.21	3.0	0.615
Warm electron (tail)	5.1×10^1	51.2	0.4	0.80
Warm electron (tail)	1.56×10^4	5464	0.4	2.0
Cold Ion (core)	2.1×10^4	0.1	1.0	0.0

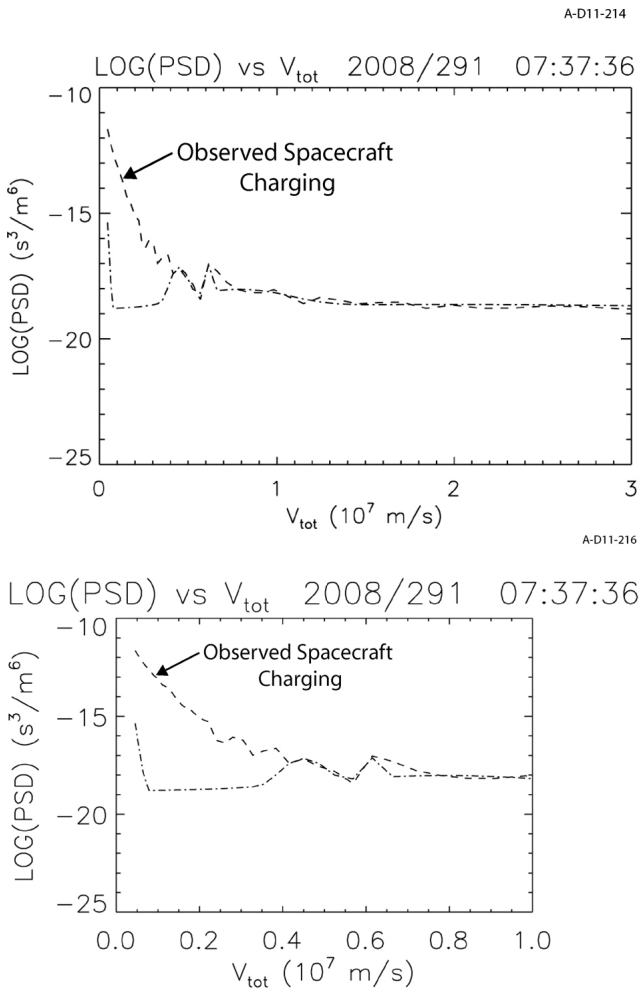

Figure 5. (top) A plot of the observed (dashed) and model (dot-dash) distribution for a pitch angle of 180 degrees (beam direction). Spacecraft charging effects are present in the observed emission for $v_{tot} \lesssim 3 \times 10^6$ m/s, so the ramped distribution observed for the lowest energies is not the actual. (bottom) A blow-up of Figure 5a showing the fit of the model distribution to the electron beam near 6.1×10^6 m/s, which is responsible for the ICW growth.

magnitude increase in wave intensity, $P/P_o = 10^6$, and we obtain $l \sim 42.4$ km. Thus growth of the ICWs can be accomplished in a very short distance. The magnetic field data indicate the presence of a weak magnetic component, but the presence of the interference resonance lines make analysis problematic.

[8] We have investigated the possible role of ion heating due to the ICWs. *Lysak et al.* [1980] studied both the linear and nonlinear heating effects of ICWs as applied to terrestrial observations. They describe ion heating with a set of ordinary differential equations,

$$dW_\perp/dt = dW_{turb}/dt - 3\ W_\perp v_\parallel/r \quad (1)$$

$$dv_\parallel/dt = 3W_\perp/(m_i r) + (e/m_i)E_\parallel \quad (2)$$

$$dW_{turb}/dt = E^2_{wave}\Omega^2\ \ \Gamma_1\ \ R_k/W_{turb} \quad (3)$$

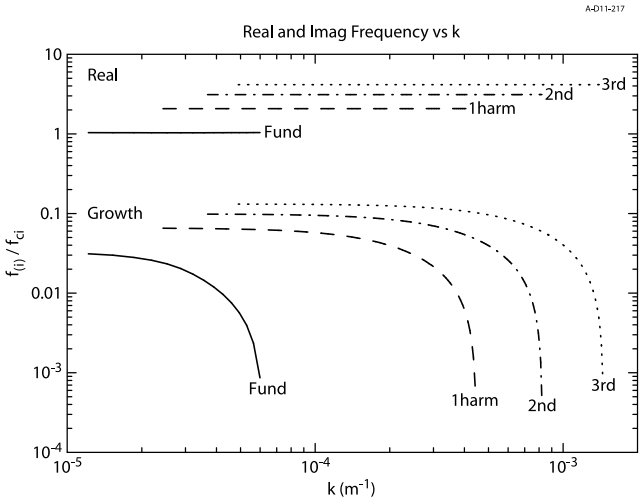

Figure 6. The real frequency (upper curves) and growth rate (lower curves) relative to $\Omega_H(f_{cH} = 5.77$ Hz) versus wave number for the fundamental and first 3 harmonics.

where $W_\perp$ is the ion perpendicular energy, $v_\parallel$ is the velocity of the electrons along the magnetic field line, r is the radial distance, m_i is the ion mass, and $E_\parallel$ is the field-aligned electric field. W_{turb} is linear perpendicular heating due to the ICW waves, with E_{wave}, the wave energy, $R_k \sim 1/\Omega$, the resonance function, and $\Gamma_1(x) = e^{-x}I_1(x) \sim 0.22$ results from the dielectric constant for EIC waves (I_1 is the modified Bessel function.) In order to obtain a sense of the possible effects of ICWs on ion heating, we integrate the above equations using the calculated linear growth rate to estimate W_{turb}. It is highly probable that a large upward electric field exists below the spacecraft, but because we have no details, we assume $E_\parallel = 0$ at least between the spacecraft and the source of the ICWs. We start the calculation at a radial distance of 4.0 R_s (R_s = Saturn radius = 60,000 km) with $W_\perp = 0.1$ eV and $v_\parallel = 3000$ m/s. This distance is

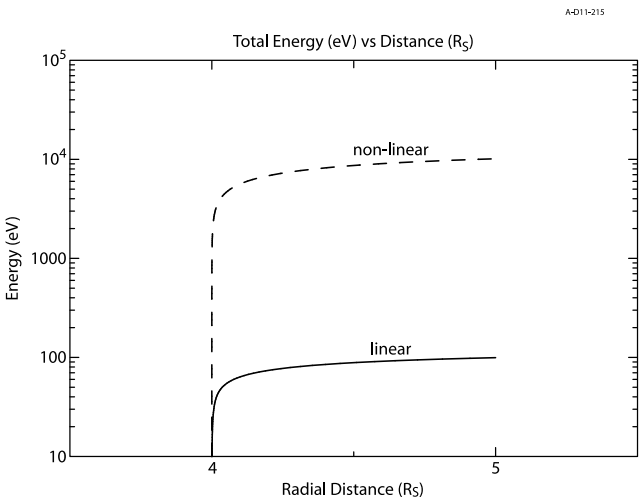

Figure 7. Ion heating versus radial distance for the case of linear (lower curve) and nonlinear process due to ion cyclotron waves.

approximately 0.5 R_s below the Cassini altitude at the time of the ICW observations. It is clear from Figure 7 that in a very short distance (relative to the radius of Saturn) ion energies increase slowly to several hundreds of eV, which are much lower than the values of the observed maximum ion energies. Only waves near the fundamental frequency were included as energy sources, because the contribution due to the harmonics would increase the total heating only slightly. It is important to note that nonlinear effects could increase this heating dramatically, perhaps by a factor of greater than 100. By recalculating W_{turb} for nonlinear growth due to electron trapping by wave potentials, *Lysak et al.* [1980] obtain coherent power levels given by

$$dW_{turb}/dt = E_{wave}\ \Omega\ \left[\left(2m_i\Omega_i^2\right)/\left(\pi^2 k_\perp^2 W_\perp\right]\right)^{1/4} \qquad (4)$$

with $k_\perp$ being the perpendicular wave number. The upper (dashed) curve of Figure 7 shows the results of replacing equation (3) with equation (4). The heating is seen to be over 2 orders of magnitude higher. These energies are comparable to those observed for the ions during the observations of the ICWs in Figure 1.

3. Summary and Conclusions

[9] Ion cyclotron waves have been observed by the Waveform Receiver (WFR) on board Cassini during a high-latitude pass of the Saturn magnetosphere. These waves are often observed on auroral passes of the terrestrial magnetosphere and are known to accelerate magnetospheric ions [cf. *Ashour-Abdalla et al.*, 1978; *Lysak et al.*, 1980; *Singh et al.*, 1981]. During a high-latitude auroral pass by Cassini on day 291 of 2008, intense upward electron beams in a downward current region were observed associated with hydrogen cyclotron waves. Ions observed at this time were weak and diffuse, probably heated by the ICWs. The electron beams are a free-energy source for growth of the observed ICWs. Growth rates of $\sim$3% Ω_H for the fundamental are calculated using a dispersion-solver (WHAMP). The observed electron phase space distribution was fit to a sum of drifting Maxwellians. These waves contain a weak magnetic component and have electric fields with a small component along the field-aligned direction. The observed magnetic component of the waves is quite noisy, however, and it is difficult to determine how much of the signal is truly electromagnetic. If some of the magnetic component is due to electromagnetic ion cyclotron modes, then interaction of these waves with the electrons may explain some of the electron energy dispersion reported by *Schippers et al.* [2011] near this time period. A more extensive examination of possible EMIC waves remains for a future study.

[10] We have investigated heating of the ions resulting from the observed ICWs. Based on the work of *Lysak et al.* [1980] we calculate linear heating of cold ions near 4 R_s up to several hundred eV at 5 R_s. These energies are a result of heating over large distances along the Saturn magnetospheric field lines as suggested by *Mitchell et al.* [2009], but are still lower than the observed ion energies of several keV. Linear heating is only considered for waves near the fundamental frequency, because the contribution due to the harmonics would increase the total heating only slightly. If nonlinear effects such as electron trapping in wave potential wells are considered, the cold ions can be heated to 10 keV, comparable to observed energies at the time. The growth of ICWs should remove a small fraction of the energy of the upward electrons beams near 100 eV, the free energy source. During the time when the waves are observed, and when the pitch angle coverage of the ELS includes upward electrons, we observe low-energy beams intermittently. Sometimes the beams show a steep gradient, df/dv_1, and sometimes with a much lower gradient, consistent with a period of active wave growth. We have assumed that there is no parallel electric field between the source of the ICWs and the Cassini spacecraft. A downward electric field below the spacecraft might actually enhance heating of ions produced by waves below the parallel electric field. It is conceivable that a field-aligned static electric field could trap the upward ions to increase the heating rate if the wave source region is below the electric field [cf. *Gorney et al.*, 1985]. Such a mechanism could explain the observed maximum ion energies to hundreds of keV for earlier and later times of this pass. Ion cyclotron waves can thus play a substantial role in the heating of auroral ions at Saturn, in much the same way that they do at Earth.

[11] **Acknowledgments.** Research at the U. of Iowa was supported by NASA through contract 1415150 with the Jet Propulsion Laboratory. JDM thanks J. Chrisinger for assistance with a number of the figures and J. Barnholdt for clerical assistance. The work at Southwest Research Institute was supported in part by NASA JPL contract 1405851.

[12] Philippa Browning thanks the reviewers for their assistance in evaluating this paper.

References

Ashour-Abdalla, M., and R. M. Thorne (1978), Toward a unified view of diffuse auroral precipitation, *J. Geophys. Res.*, *83*(A10), 4755–4766, doi:10.1029/JA083iA10p04755.

Bunce, E. J., S. W. H. Cowley, D. L. Talboys, L. Lamy, W. S. Kurth, P. Schippers, B. Cecconi, P. Zarka, C. S. Arridge, and A. J. Coates (2010), Extraordinary field-aligned current signatures in Saturn's high-latitude magnetosphere: Analysis of Cassini data during Revolution 89, *J. Geophys. Res.*, *115*, A10238, doi:10.1029/2010JA015612.

Carlson, C. W., et al. (1998), FAST observations in the downward auroral current region: Energetic upgoing electron beams, parallel potential drops, and ion heating, *Geophys. Res. Lett.*, *25*(12), 2017–2020, doi:10.1029/98GL00851.

Cattell, C., et al. (1998), The association of electrostatic ion cyclotron waves, ion and electron beams and field-aligned currents: FAST observations of an auroral zone crossing near midnight, *Geophys. Res. Lett.*, *25*(12), 2053–2056, doi:10.1029/98GL00834.

Chaston, C. C., et al. (1998), Characteristics of electromagnetic proton cyclotron waves along auroral field lines observed by FAST in regions of upward current, *Geophys. Res. Lett.*, *25*(12), 2057–2060, doi:10.1029/98GL00513.

Chaston, C. C., J. W. Bonnell, J. P. McFadden, R. E. Ergun, and C. W. Carlson (2002), Electromagnetic ion cyclotron waves at proton cyclotron harmonics, *J. Geophys. Res.*, *107*(A11), 1351, doi:10.1029/2001JA900141.

Gorney, D. J., Y. T. Chiu, and D. R. Croley Jr. (1985), Trapping of ion conics by downward parallel electric fields, *J. Geophys. Res.*, *90*(A5), 4205–4210, doi:10.1029/JA090iA05p04205.

Gurnett, D., and L. Frank (1972), ELF noise bands associated with auroral electron precipitation, *J. Geophys. Res.*, *77*(19), 3411–3417, doi:10.1029/JA077i019p03411.

Kindel, J. M., and C. F. Kennel (1971), Topside current instabilities, *J. Geophys. Res.*, *76*(13), 3055–3078, doi:10.1029/JA076i013p03055.

Kintner, P. M., M. C. Kelley, and F. S. Mozer (1978), Electrostatic hydrogen cyclotron waves near one Earth radius altitude in the polar magnetosphere, *Geophys. Res. Lett.*, *5*(2), 139–142, doi:10.1029/GL005i002p00139.

Kurth, W. S., et al. (2011), A close encounter with a Saturn kilometric radiation source region, in *Planetary Radio Emissions VII*, edited by H. O. Rucker et al., Austrian Acad. of Sci. Press, Vienna, in press.

Lamy, L., et al. (2010), Properties of Saturn kilometric radiation measured within its source region, *Geophys. Res. Lett.*, *37*, L12104, doi:10.1029/2010GL043415.

Lin, C. S., H. K. Wong, J. Koga, and J. L. Burch (1989), Excitation of low-frequency waves by auroral electron beams, *J. Geophys. Res.*, *94*(A2), 1327–1337, doi:10.1029/JA094iA02p01327.

Lund, E. J., et al. (1998), FAST observations of preferentially accelerated He+ in association with auroral electromagnetic ion cyclotron waves, *Geophys. Res. Lett.*, *25*(12), 2049–2052, doi:10.1029/98GL00304.

Lysak, R. L., M. K. Hudson, and M. Temerin (1980), Ion heating by strong electrostatic ion cyclotron turbulence, *J. Geophys. Res.*, *85*(A2), 678–686, doi:10.1029/JA085iA02p00678.

McFadden, J. P., et al. (1998), Electron modulation and ion cyclotron waves observed by FAST, *Geophys. Res. Lett.*, *25*(12), 2045–2048, doi:10.1029/98GL00855.

Mitchell, D. G., W. S. Kurth, G. B. Hospodarsky, N. Krupp, J. Saur, B. H. Mauk, J. F. Carbary, S. M. Krimigis, M. K. Dougherty, and D. C. Hamilton (2009), Ion conics and electron beams associated with auroral processes on Saturn, *J. Geophys. Res.*, *114*, A02212, doi:10.1029/2008JA013621.

Ronnmark, K. (1982), WHAMP waves in a homogeneous anisotropic multicomponent plasma, *Rep. 179*, Kiruna Geophys. Inst., Kiruna, Sweden.

Ronnmark, K. (1983), Computation of the dielectric tensor of a Maxwellian plasma, *Plasma Phys.*, *25*(6), 699–701, doi:10.1088/0032-1028/25/6/007.

Rosenbluth, M. N. (1965), *Microinstabilities in Plasma Physics*, pp. 585–594, Int. At. Energy Agency, Vienna.

Schippers, P., et al. (2011), Auroral electron distributions within and close to the Saturn kilometric radiation source region, *J. Geophys. Res.*, *116*, A05203, doi:10.1029/2011JA016461.

Singh, N., R. W. Schunk, and J. J. Sojka (1981), Energization of ionospheric ions by electrostatic hydrogen cyclotron waves, *Geophys. Res. Lett.*, *8*(12), 1249–1252, doi:10.1029/GL008i012p01249.

Singh, N., J. R. Conrad, and R. W. Schunk (1985), Electrostatic ion cyclotron, beam-plasma, and lower hybrid waves excited by an electron beam, *J. Geophys. Res.*, *90*(A6), 5159–5172, doi:10.1029/JA090iA06p05159.

Temerin, M., and R. L. Lysak (1984), Electromagnetic ion cyclotron mode (ELF) waves generated by auroral electron precipitation, *J. Geophys. Res.*, *89*(A5), 2849–2859, doi:10.1029/JA089iA05p02849.

Temerin, M., J. McFadden, M. Boehm, C. W. Carlson, and W. Lotko (1986), Production of flickering aurora and field-aligned electron flux by electromagnetic ion cyclotron waves, *J. Geophys. Res.*, *91*(A5), 5769–5792, doi:10.1029/JA091iA05p05769.

Weibel, E. S. (1970), Ion cyclotron instability, *Phys. Fluids*, *13*(12), 3003, doi:10.1063/1.1692893.

Young, D. T., et al. (2004), Cassini Plasma Spectrometer Investigation, *Space Sci. Rev.*, *114*(1–4), 1–112, doi:10.1007/s11214-004-1406-4.

A. J. Coates, Mullard Space Science Laboratory, University College London, London RH5 6NT, UK.

F. Crary, Southwest Research Institute, PO Drawer 28510, San Antonio, TX 78229, USA.

D. A. Gurnett, J. D. Menietti, and P. Schippers, Department of Physics and Astronomy, University of Iowa, 210 Van Allen Hall, Iowa City, IA 52242-1479, USA. (john-menietti@uiowa.edu)

O. Santolík, Faculty of Mathematics and Physics, Charles University, V Holesovickach 2, 18000 Prague 8, Czech Republic.